Anisotropy of the upper critical fields and the paramagnetic Meissner effect in $La_{1.85}Sr_{0.15}CuO_4$ single crystals

2013 J. Phys.: Condens. Matter 25 065702

(http://iopscience.iop.org/0953-8984/25/6/065702)

J. Phys.: Condens. Matter **25** (2013) 065702 (7pp) doi:10.1088/0953-8984/25/6/065702

Anisotropy of the upper critical fields and the paramagnetic Meissner effect in $La_{1.85}Sr_{0.15}CuO_4$ single crystals

I Felner[1], M I Tsindlekht[1], G Drachuck[2] and A Keren[2]

[1] Racah Institute of Physics, The Hebrew University, Jerusalem, 91904, Israel
[2] Department of Physics, Technion-Israel Institute of Technology, Haifa, 32000, Israel

E-mail: israela@mail.huji.ac.il

Received 23 October 2012, in final form 14 December 2012
Published 11 January 2013
Online at stacks.iop.org/JPhysCM/25/065702

Abstract

Optimally doped $La_{1.85}Sr_{0.15}CuO_4$ single crystals have been investigated by dc and ac magnetic measurements. These crystals have rectangular needle-like shapes with the long needle axis parallel to the crystallographic c axis (c-crystal) or parallel to the basal planes (a-crystal). In both crystals, the temperature dependence of the upper critical fields (H_{C2}) and the surface critical field (H_{C3}) were measured. The H–T phase diagram is presented. Close to $T_C = 35$ K, for the c-crystal, $\gamma^c = H^c_{C3}/H^c_{C2} = 1.80(2)$, whereas for the a-crystal the $\gamma^a = H^a_{C3}/H^a_{C2} = 4.0(2)$ obtained is much higher than 1.69, predicted by the ideal mathematical model. At low applied dc fields, positive field-cooled branches known as the 'paramagnetic Meissner effect' (PME) are observed; their magnitude is inversely proportional to H. The anisotropic PME is observed in both a- and c-crystals, only when the applied field is along the basal planes. It is speculated that the high γ^a and the PME are connected to each other.

(Some figures may appear in colour only in the online journal)

1. Introduction

Bulk superconductivity (SC) in type-II superconductors appears when the applied magnetic field (H) is lower than the upper critical field H_{C2}. For optimally doped $La_{1.85}Sr_{0.15}CuO_4$ (LSCO, $T_C \sim 35$ K) and $YBa_2Cu_3O_{7-\delta}$ (YBCO, $T_C \sim 92$ K) single crystals, the temperature dependence of H_{C2} has been extensively studied only close to T_C, but their low temperature behaviour has not been fully understood. This is mainly due to the fact that, at low temperatures, their normal state can be accessed only by magnetic fields higher than 50 T. Ultra high magnetic fields can be generated only for a short duration (less than 10 ms), therefore conventional resistivity measurements are extremely difficult. The first low-temperature study on YBCO up to 250 T for a magnetic applied field (H) parallel to the CuO_2 (ab) planes has been performed only very recently [1]. The constructed field–temperature phase diagram for YBCO, over a wide temperature range, yields $H_{C2} = 240$ T at 5 K (see [1] and in references therein). In contrast to YBCO, very few studies have been reported on $H_{C2}(T)$ of LSCO single crystals and it was found that H_{C2} is anisotropic. H_{C2} for H parallel to the ab plane (H^a_{C2}) is higher than for H parallel to the c axis (H^c_{C2}) [2]. The estimated values for LSCO of $H^a_{C2}(0)$ and $H^c_{C2}(0)$ are 28 and 5.18 T respectively, thus the anisotropy ratio is 5.40 [3].

It is well accepted that, for H applied parallel to the sample surface, the transition to the SC state takes place at $H < H_{C3}$. For a single band superconductor, the theoretical ratio $\gamma = H_{C3}/H_{C2}$ predicted by Saint-James and De Gennes in 1963 is: ≈1.69 [4]. That means that the nucleation field of a thin SC sheet at the surface, with a thickness of the order of the Ginzburg–Landau coherence length, is higher than the nucleation field of the bulk. Experiments on the conventional SC have confirmed that γ is ∼1.81 [5]. It turns out that γ depends strongly on temperature and on boundary conditions [6, 7]. So far, to our best knowledge, the surface superconducting state (SSS) in $La_{1.85}Sr_{0.15}CuO_4$ has not

yet been studied. On the other hand, for the new layered $K_{0.73}Fe_{1.68}Se_2$ SC single crystal (for $H \parallel ab$), the temperature dependence of H_{C3} and H_{C2} yields $\gamma \sim 4.4$, a value which is much larger than the predicted $\gamma = 1.69$ discussed above [8].

The Meissner effect, the expulsion of magnetic flux when a superconductor is placed in a magnetic field and cooled down through its T_C in the field-cooled (FC) process, is arguably the fingerprint of the SC state. Surprisingly, it was shown that at low H only, some SC materials may attract the magnetic field. It means that positive magnetization signals appear via the FC procedure, a phenomenon known as the paramagnetic Meissner (PME) or the Wohlleben effect [9]. Observation of the PME has been reported: in single crystals, in sintered and melt-textured polycrystalline samples as well as in thin films of Cu–O based superconductors. In YBCO single crystal the PME is small and was observed only for $H \parallel c$ [10, 11], whereas in multilayered $YBa_2Cu_3O_7/La_{0.7}Ca_{0.3}MnO_3$ (YBCO/LCMO) films a pronounced effect was observed for $H \parallel ab$ [12]. On the other hand in powder Bi-2212, the positive magnetic susceptibility reaches 60% of the complete diamagnetic Meissner effect [13]. Typically, the PME is observed in a relatively small number of measured samples. The scarce experimental evidence makes it difficult to identify the origin of this enigmatic phenomenon, although a large number of possible explanations for PME have been advanced [14, 15]. Although it is possible that the proposed mechanisms do play a role in high-T_C superconductors, more recent observations of PME in Nb [16, 17] clearly indicate the existence of another, less-exotic mechanism [18]. The limited choice of assumptions in this case makes the origin of PME more mysterious.

The theory for conventional SC employs that the PME originates from flux capture (caused by in-homogeneities) inside a SC sample and its consequent compression with decreasing temperature [18]. Alternatively, PME could also be an intrinsic property of any finite-size superconductor due to the presence of sample boundaries. The PME is explained by the giant vortex state with fixed orbital moment. Compressing the magnetic flux trapped by this vortex state can lead to the PME [19]. A more recent theoretical model, which is distinct from the previous ones, assumes that the PME is caused by impurities (such as oxygen vacancies) and the localized moments of the two-level system found in HTSC. This two-level system is created by the surplus oxygen atom and a neighbouring oxygen vacancy, united by a common singlet electron pair, and their moment produces the PME effect [20]. For the super-lattice YBCO/LCMO system, PME is observed for samples whose LCMO layers are magnetically granular, indicating that surface pinning effect are at the root of PME [12].

In this paper we report an experimental study of optimally doped SC $La_{1.85}Sr_{0.15}CuO_4$ single crystals ($T_C = 35$ K). They were cut to rectangular needle-like shapes with the long needle axis parallel to the crystallographic c-axis or parallel to the ab basal plane, assigned as 'c' and 'a' crystals respectively, as depicted in figure 1 (inset). The resistivity and the low-field susceptibility measurements of

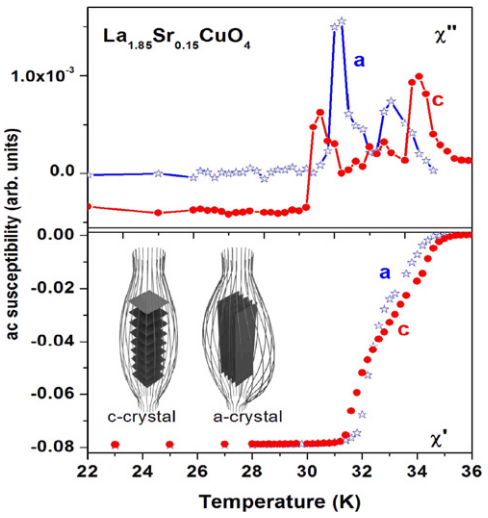

Figure 1. Temperature dependences of real (χ') and imaginary (χ'') components of the ac susceptibility of a- and c $La_{1.85}Sr_{0.15}CuO_4$ crystals measured at 1465 Hz at $H = 0$. For the sake of clarity, the two (χ'') curves were shifted from each other. The inset shows the schematic orientation of the two a- and c- crystals [21]. The grey lines illustrate schematically the external field lines.

both crystals clearly indicate anisotropy in the temperature at which the magnetization is detectable, and also anisotropy in the temperature at which zero resistivity appears [21]. For the same two 'a' and 'c' $La_{1.85}Sr_{0.15}CuO_4$ crystals, dc and ac magnetic measurements for H parallel to the long dimension of the crystals have been performed, from which the $H_{C2}(T)$ and $H_{C3}(T)$ curves were deduced. The major findings reported here are: (i) it is shown that, near T_C, for the c-crystal $\gamma^c = H^c_{C3}/H^c_{C2}$ is 1.8(2), a value which is in fair agreement with the theoretical 1.69 ratio [4]. On the other hand, for the a-crystal the high $\gamma^a = H^a_{C3}/H^a_{C2} = 4.0(2)$ obtained is very similar to that observed in the layered $K_{0.73}Fe_{1.68}Se_2$ measured in the same geometry [8]. (ii) We demonstrate anisotropic PME in both a- and c- crystals. Positive FC signals are observed only when H is along the basal planes ($H \parallel ab$), whereas for $H \parallel c$ the usual negative Meissner state is obtained. It is speculated that these two new phenomena, namely, the high γ^a ratio and the PME for $H \parallel ab$ only, are inter-connected to each other and have basically the same origin.

2. Experimental details

A relatively large optimally doped $La_{1.85}Sr_{0.15}CuO_4$ single crystal has been grown in an image furnace. The crystal was oriented with an x-ray Laue camera, and then cut to rectangular needle-like shapes with the long needle axis parallel to the ab basal planes (a-crystal) or parallel to the crystallographic c- axis (c-crystal) [21]. The abc dimensions of these crystals are: 1.8 mm × 2.3 mm × 8.5 mm and 1.7 mm × 2.0 mm × 3.2 mm respectively. The compositions, as well as the homogeneity of the crystals, were studied by various methods as described in [21]. The dc magnetic studies were done in a commercial MPMS5 Quantum Design superconducting quantum interface device

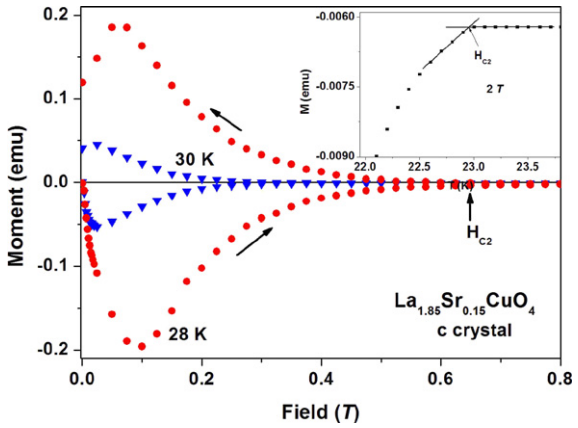

Figure 2. Two isothermal dc magnetic hysteresis loops measured at 28 and 30 K for the c-crystal and the $M(T)$ plot measured at 2 T (inset), from which $H^c_{C2}(T)$ is deduced.

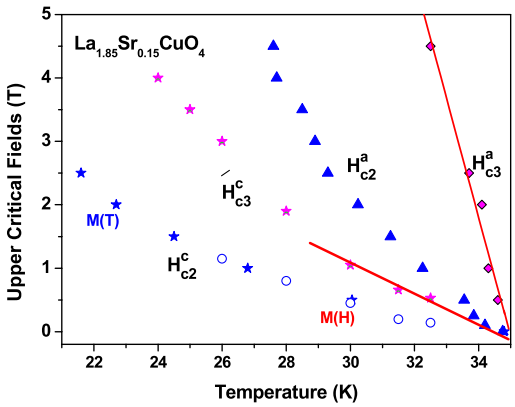

Figure 3. Temperature dependence of the upper and surface critical magnetic fields: H^a_{C2} and H^a_{C3}, and H^c_{C2} and H^c_{C3}. Note the almost linear plots near T_C of all four curves. The H^c_{C2} curve was obtained by $M(T)$ (filled) and $M(H)$ (open) methods (see text).

(SQUID) magnetometer. The real (χ') and imaginary (χ'') ac susceptibilities were measured with a home-made pickup coil method at amplitude of $h_0 = 0.05$ Oe at various frequencies up to $\omega/2\pi = 1465$ Hz. The crystals were inserted into one of a balanced pair of coils, and the unbalanced signal was measured by a lock-in amplifier. The setup was adapted to the SQUID magnetometer, as described in detail in [22]. All the ac susceptibility data presented here were collected when the dc field was applied parallel to the crystals' long needle axis.

3. Experimental results

Real (χ') and imaginary (χ'') ac susceptibility measurements have been performed on both a- and c-crystals at several frequencies under various applied dc fields. Both χ' and χ'' signals are unaffected by the frequency. Thus, the plots obtained at low frequencies and at 1465 Hz were identical. Figure 1 shows the χ' and χ'' curves measured at 1465 Hz at dc zero field. The onset of χ' signals at $T_C = 34.8(1)$ and 35.4(1) K for a- and c-crystals respectively, are in good agreement with $T_C = 35$ K, deduced from resistivity and low-field dc magnetization data presented in [21]. The relatively broad transitions may indicate a small spread in stoichiometry along the crystals. This assumption is consistent with the double peaks observed in the χ'' curve at 31.6 and 33.6 K for the a-crystal and at 32.2 and 34.4 K for the c-crystal. Alternatively, the two steps in both χ' and χ'' may be attributed to a different T_C of the bulk and the surface, as discussed later.

3.1. Determination of $H_{C2}(T)$

The criterion for determining the upper critical field $H_{C2}(T)$ requires consistency, and no method is entirely unambiguous. In many publications $H_{C2}(T)$ was deduced from resistivity and/or from ac susceptibility measurements. In high-T_C SC (HTSC) thin crystals, these studies provide accurate $H_{C2}(T)$ values only when H is perpendicular to the wide sample surface [7]. In this geometry the bulk nucleation of SC starts indeed at $H < H_{C2}$. On the other hand, for H parallel to the wide surface, $H_{C2}(T)$ can be deduced from bulk measurements, such as dc $M(H)$ and/or $M(T)$, as well as from specific heat studies.

Here, $H^a_{C2}(T)$ and $H^c_{C2}(T)$ were determined by using two complementary methods. The isothermal field dependence of the dc magnetization $M(H)$ has been measured at various temperatures. Two typical hysteresis loops measured at 28 and 30 K are presented in figure 2. H_{C2} (indicated by the vertical arrow) was defined as the field at which the two ascending and descending curves merge. Alternatively, the temperature dependence of the magnetization $M(T)$ under various applied fields has been measured and $H_{C2}(T)$ was determined at the crossing point, as shown in figure 2 (inset). The two methods yield practically the $H^c_{C2}(T)$ curves, as presented in figure 3.

It is well accepted that, in HTSC, the strong thermal fluctuations as well as the short coherence length may obscure the real bulk H_{C2} transitions, thus one may argue that the $H_{C2}(T)$ curves presented in figure 3 are in fact the irreversibility lines. We argue that in our $M(T)$ plots, the irreversibility transitions, defined as the merging temperature of the ZFC and FC branches, lie below the onset of the diamagnetic signals, as shown later in figure 6(a) for $H \parallel c$ of the c-crystal. Therefore, we tend to believe that the H^c_{C2} line, which basically was deduced from the $M(T)$ curves, represents the bulk H_{C2} line. It is reasonable to assume that the same procedure holds for the second orientation.

A rough estimation of $H_{C2}(0)$ can be achieved by using the well-known Werthamer–Helfand–Hohenberg (WHH) relation: $H_{C2}(0) = -0.69T_C(\mathrm{d}H_{C2}/\mathrm{d}T)$ [23], where the T_C values are listed above. The linear slopes (near T_C) are $-0.48(1)$ and $-0.17(1)T/K$ and the estimated $H^a_{C2}(0)$ and $H^c_{C2}(0)$ values are 11.6(1) and 4.1(1) T for a- and c-crystals respectively. This yields the anisotropy of $H^a_{C2}(0)/H^c_{C2}(0) = 2.8(2)$. It should be noted that the WHH equation is just a rough estimation for $H_{C2}(0)$. An accurate value can only be achieved by applying high enough magnetic fields. The value obtained for $H^c_{C2}(0)$ is in fair agreement with $H^c_{C2}(0) = 5.2$ T for LSCO in the same geometry [3]. On the other

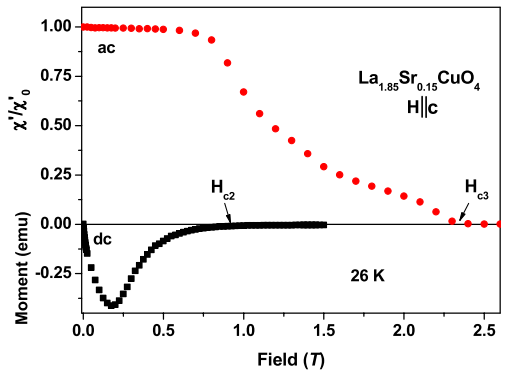

Figure 4. A comparison between the dc magnetization and the normalized ac χ' susceptibility measured at 26 K under the same experimental conditions for $H \parallel c$ of the c-crystal, from which H_{C2} and H_{C3} are deduced.

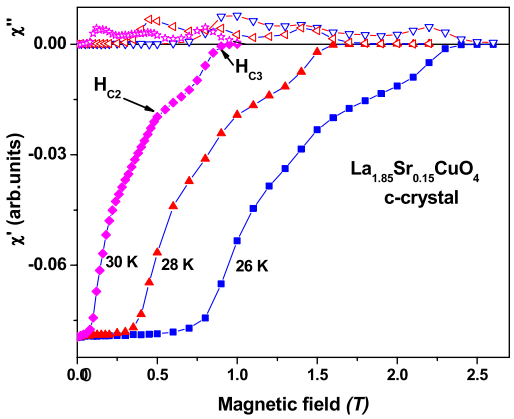

Figure 5. Isothermal field dependence of the real and imaginary ac susceptibility branches of the c-crystal measured at 26, 28, 30 K, from which $H^c_{C3}(T)$ was deduced.

hand, our $H^a_{C2}(0)$ is much smaller than 28 T [24] and 75 T [3]. Since the method to determine $H_{C2}(0)$ in [3] is not reported, we may suspect that the high $H^a_{C2}(0)$ obtained is rather the third critical field, $H^a_{C3}(0)$. Due to the limited number of publications on $H_{C2}(T)$ for $La_{1.85}Sr_{0.15}CuO_4$, any further discussion is needless. We also encourage a revised estimation of the already reported $H_{C2}(T)$ values in other HTSC materials.

3.2. Determination of $H_{C3}(T)$

The $H_{C3}(T)$ values were obtained from ac susceptibility studies measured at various frequencies up to 1465 Hz. A comparison between the ascending dc $M(H)$ plot and the normalized χ' (measured at 1465 Hz) for $H \parallel c$ of the c-crystal at 26 K, is shown in figure 4. As stated above, the dc curve yields the H_{C2} value. It is readily observed that χ', although measured under the same conditions, becomes zero at higher H (our determination for H_{C3}). This demonstrates clearly the presence of SC at $H > H_{C2}$. Figure 5 depicts the real and imaginary ac plots of the c-crystal (for $H \parallel c$) at three typical temperatures, from which the $H^c_{C3}(T)$ curve in figure 3 was constructed. The same approach was applied to the a-crystal.

Here again, near T_C, both $H^a_{C3}(T)$ and $H^c_{C3}(T)$ plots are almost linear, with the slopes of $dH_{C3}/dT = -1.95(1)$ and $-0.31(1)T/K$ respectively. This indicates that $\gamma^a = H^a_{C3}/H^a_{C2} = 4.0(2)$ and $\gamma^c = H^c_{C3}/H^c_{C2} = 1.8(2)$. Within the uncertainty values, this γ^c fits well the predicted $\gamma = 1.69$ as discussed above [4]. On the other hand, the unexpectedly high γ^a value is very similar to that obtained for the same orientation in the layered $K_{0.73}Fe_{1.68}Se_2$ crystal [8].

To the best of our knowledge, no theory exists for such high γ^a in LSCO. This high γ^a cannot be explained by the multiband structure and standard boundary conditions of the order parameter, because for this model γ^a does not exceed 1.75, as demonstrated in our previous publication [25]. We may speculate that non-standard boundary conditions of the order parameter are needed to explain this phenomenon [7].

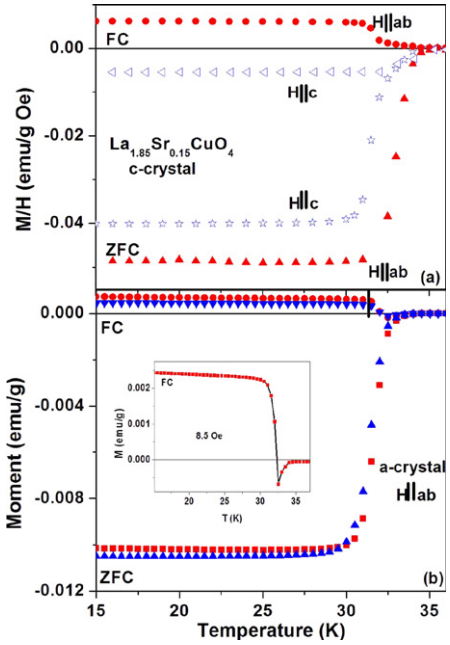

Figure 6. (a) ZFC and FC susceptibility plots of the c-crystal for H applied parallel and perpendicular to the c-axis measured at 2.3 and 1.4 Oe respectively. (b) ZFC and FC magnetization curves of the a-crystal, measured at 3.5 (blue) and 5.5 Oe (red) for H parallel to the long axis. The inset shows the FC plot measured at 8.5 Oe.

3.3. The paramagnetic Meissner effect (PME)

The c-crystal. The dc ZFC and FC magnetization curves of the c-crystal were measured parallel (at 2.3 Oe) and perpendicular (at 1.4 Oe) to the longer c-axis. Figure 6(a) shows the normalized (M/H) ZFC and FC branches obtained in both orientations. As expected, the two ZFC branches are diamagnetic. Due to the different demagnetization factors (not calculated) the shielding fractions in the two directions are slightly different. On the other hand, in the FC process, for $H \parallel c$ the expected diamagnetic Meissner state below T_C is obtained, whereas for $H \parallel ab$ the signals are positive. This,

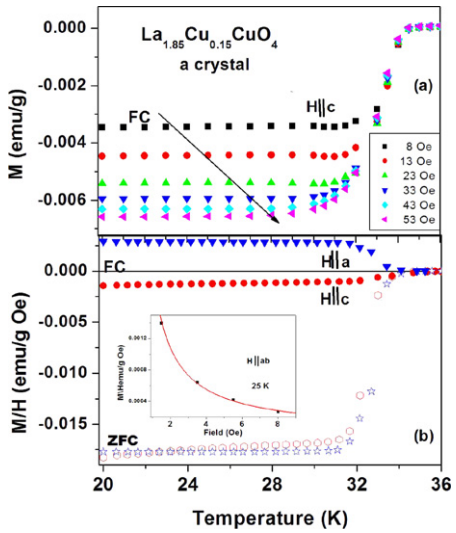

Figure 7. (a) FC plots of the *a*-crystal for $H \parallel c$. (b) The normalized ZFC and FC plots of the *a*-crystal measured perpendicular to the long axis, for H parallel and perpendicular to the *ab* planes measured at 4 Oe (red) and 2.5 Oe (blue) respectively. The inset shows the field dependence of the PME effect for $H \parallel a$.

anisotropy indicates that a PME is obtained for the $H \parallel ab$ direction only. It is worth noting that increasing the cooling rate by an order of magnitude did not affect the PME signals. The shielding fraction deduced from the ZFC branch (for $H \parallel ab$) accounts for 96%, indicating a rather perfect bulk superconductor. As a controlled experiment, we have crushed one of crystals into powder and measured the ZFC and FC curves at low H. As expected, all FC branches are negative, as depicted for the $H \parallel c$.

The a-crystal. For the *a*-crystal for $H \parallel ab$ (the long dimension), the FC branches are positive, thus the same PME is observed (figure 6(b)). After tracing the FC process at 3.5 Oe, the system was cooled back to 12 K and then H was switched off. The positive remnant moments (not shown) measured up to T_C are ∼14 times higher than the positive FC signals shown in figure 6(b) and are quite similar to the absolute ZFC values. To confirm the PME observation, we measured the *a*-crystal along its two short dimensions. In contrast to the *c*-crystal, for H applied perpendicular to the long dimension, two possibilities are present. (i) H may be applied along the shortest dimension (1.8 mm), which is the crystallographic *c*-axis. (ii) Alternatively H may be applied parallel to the middle dimension (2.2 mm), which is the *ab* basal plane. Figure 7(a) shows that in the first case, for $H \parallel c$, all FC curves obtained measured up to $H = 53$ Oe are negative, exhibiting the regular typical Meissner effect. On the other hand, in the second case, for $H \parallel ab$, the PME phenomenon is readily observed (figure 7(b)). This definitely proves that in both *a*- and *c*-crystals, the PME is observed only when H is applied along the basal planes. This behaviour is perfectly reproducible. We also measured a second *a*-crystal and obtained similar results.

Remarkably, the observed PME in various SC systems, which appears only at very low H values (less than 1 Oe), is exhibited here up to H of ∼10–15 Oe. For the *a*-crystal, the positive M/H (measured at 25 K along the long dimension) decreases with H as $M/H = C^*H^{-\alpha}$, where the constant $C = 0.0021$ and $\alpha = 1.0 \pm 0.05$, indicating that the M/H is inversely proportional to H (figure 7(b) inset). Moreover, due to the similarity in the short and middle dimensions, we may assume that the demagnetization factor in both directions is very similar, thus we may compare between the normalized positive and negative signals presented in figure 7(b). As expected, the two ZFC curves in both directions are quite similar. On the other hand, in the FC branches, the positive PME signal is twice as much as in the diamagnetic one.

We conclude that in all our LSCO crystals, (i) the PME is observed only for $H \parallel ab$, (ii) the positive signal is larger than the Meissner state. This observation differs strictly from that reported for YBCO crystal, where the PME signal is small and was observed only for $H \parallel c$ [13].

4. Discussion

Two important physical parameters of the optimal doped $La_{1.85}Sr_{0.15}CuO_4$ single crystal are addressed here: (i) we show the H–T phase diagram, which includes the upper critical fields $H_{C2}(T)$ and $H_{C3}(T)$ for both $H \parallel c$ and $H \parallel ab$ orientations; (ii) the PME phenomenon which is observed only for $H \parallel ab$. To our best knowledge, these observations are reported for the first time.

(i) In contrast to YBCO, only a limited number of publications have reported on the upper critical field of optimally doped LSCO crystals [2, 3, 24, 26]. Due to the lack of large single crystals most of the published results report mainly on the doping dependence of $H_{C2}(T)$ along the *c*- axis. It is well accepted that $H_{C2}(T)$ is anisotropic and that $H^a_{C2} > H^c_{C2}$, however the anisotropy ratio 2.8(2) presented here is smaller than 5.4 reported in [3]. By using the ac susceptibility technique, we studied the surface critical magnetic fields $H_{C3}(T)$ and deduced the ratio $\gamma = H_{C3}/H_{C2}$ in both $H \parallel c$ and $H \parallel ab$ directions. $\gamma^c = 1.8(2)$ fits well the theoretical 1.69 value. On the other hand, a much higher $\gamma^a = 4.0(2)$ is obtained.
One may argue that the higher γ^a obtained is caused by the inhomogeneity of the measured crystals (see figure 1) due to the spread in stoichiometry. Indeed, it is very rare to find large single crystals (3.2 and 8.5 mm long) which contain four elements and are homogeneous at a microscopic level. The question is on whether the data presented are affected by this inhomogeneity. As mentioned above, the criterion for determining the upper critical field $H_{C2}(T)$ requires consistency, and no method is entirely unambiguous. Here, we use the same criterion to define $H_{C2}(T)$ along and perpendicular to the basal planes. Therefore, this inhomogeneity should affect simultaneously the two $H_{C2}(T)$ values measured in these directions. The fact that γ^c obtained fits well the Saint-James–de Gennes theoretical value, but γ^a does not, may clearly indicate that the difference between the γ values is an intrinsic property of LSCO.

In addition, one may argue that the deduced $H_{C2}(T)$ values are not the upper critical fields but rather the irreversibility lines, which always lie below the $H_{C2}(T)$ curves in the H–T phase diagram. Figure 6(a) shows that the irreversibility transition, defined as the merging temperature of the ZFC and FC branch, is below the onset of the diamagnetic signals. Therefore, we tend to believe that curves presented in figure 3 are the $H_{C2}(T)$ lines. Moreover, it is well accepted that at low external fields the irreversibility and the $H_{C2}(T)$ lines are very close to each other. Thus, if the curves shown in figure 3 are the irreversibility lines, their deduced slopes may be considered with high confidence as very similar to the slopes of the $H_{C2}(T)$ lines. Thus our determination should not change significantly the high γ^a obtained. It should be noted that γ depends strongly on the boundary conditions of the order parameter and the surface roughness [27, 28]. The question on whether these parameters are responsible for the two γ values of LSCO is still open.

(ii) The theoretical models of the PME were discussed earlier in several publications [18–20]. There is no consensus as to what are the essential factors which cause the PME. It is proved here that for LSCO this anisotropic phenomenon is observed only when H is parallel to the Cu–O planes, regardless of whether it is measured parallel to the long (a-crystal) or to the short (c-crystal) dimension of the crystal. Moreover, figure 7 shows that, perpendicular to the long dimension of the a-crystal, the PME is observable for $H \parallel ab$ only, but not $H \parallel c$, although the demagnetization factors for both directions are almost the same. That excludes the assumption that demagnetization effects enhance the PME [14] or that the PME is caused by impurities which act as effective pinning centres for the vortices [20]. Worth mentioning, in contrast to YBCO single crystals [10, 11], in LSCO, the PME signal is larger than the negative Meissner branch (figure 6).

The theoretical model for the PME is beyond the scope of the present study. However, we may suggest that the two phenomena observed, namely, the higher γ^a ratio and the PME for $H \parallel ab$ only, are practically related to each other. Since in the layered LSCO SC is confined to the Cu–O planes, $H^c_{C2} = \Phi_0/2\pi\xi^2_{ab}$. There, as for $H \parallel ab$, H^a_{C2} depends on SC and non-SC layers (figure 1, inset) and therefore, $H^a_{C2} = \Phi_0/2\pi\xi_{ab}\xi_c$. Φ_0 is the magnetic flux quantum and ξ_{ab}, ξ_c are the coherence lengths parallel to the Cu–O planes and to the c- axis respectively. Thus, the fact that $H^a_{C2} > H^c_{C2}$ is caused by the intrinsic anisotropy of the coherence lengths ($\xi_{ab} > \xi_c$). We may speculate that for $H \parallel ab$, these two coherence lengths cause two types of induced currents, which are exhibited by the PME and by the higher γ^a value. This is in line with the model which connects the PME in Nb to the surface superconductivity, when T_C of the surface is different from that of the bulk [6, 17]. However, the current state of experiments does not allow us to suggest any consistent explanation for these anisotropies. It is possible that there is some interplay between them, but no existing theoretical models that would be able to explain these magnetic phenomena have been proposed. We encourage the development of a new model which will take these observations into account.

In summary, we have demonstrated the existence of surface superconductivity in rectangular needle-like shapes of $La_{1.85}Sr_{0.15}CuO_4$ single crystals. DC magnetization measurements yield an anisotropic ratio of 2.8(2) of the bulk upper critical fields $H_{C2}(0)$ when measured along the basal planes and the c-axis. From the ac susceptibility study we have deduced the surface magnetic critical field $H_{C3}(T)$. In the c-axis direction $H^c_{C3}/H^c_{C2} = 1.8(2)$, a value which is in fair agreement with the theoretical 1.69 ratio. On the other hand, an unexpected high ratio $H^a_{C3}/H^a_{C2} = 4.0(2)$ is obtained in the Cu–O planes. In addition, we observed an anisotropic PME. Positive FC branches were obtained only for H parallel to the Cu–O basal planes, regardless of the dimension of the crystal. It is speculated that the two anisotropies are connected to each other.

Acknowledgments

The research in Jerusalem and in the Technion is supported in part by the Israel Science Foundation ISF (389/09), ISF Bikura grant (459/09), the German-Israel DIP programme and by the Klachky Foundation for Superconductivity. MIT thanks V M Genkin for valuable discussions.

References

[1] Sekitani1 T, Matsuda Y H and Miura N 2007 *New J. Phys.* **9** 47
[2] Khlopkin M N, Panova O Kh, Chernoplekov N A, Shikov A A and Suetin A V 1997 *JETP* **85** 755
[3] Varshney D, Singh R K and Shah S 1996 *J. Supercond.* **9** 319
[4] Saint-James D and De Gennes P 1963 *Phys. Lett.* **7** 306
[5] Rollins R and Silcox J 1967 *Phys. Rev.* **155** 404
[6] Hopkins J R and Finnemore D K 1974 *Phys. Rev.* B **9** 108
[7] Tsindlekht M I, Leviev G I, Genkin V M, Felner I, Paderno Yu B and Filippov V B 2006 *Phys. Rev.* B **73** 104507
[8] Tsindlekht M I, Felner I, Zhang M, Wang A F and Chen X H 2011 *Phys. Rev.* B **84** 052503
[9] Braunisch W, Knauf N, Kataev V, Neuhausen S, Grutz A, Kock A, Roden B, Khomskii D and Wohllben D 1992 *Phys. Rev. Lett.* **68** 1908
[10] Lucht R, Löhneysen H V, Claus H, Kesler M and Müller-Vogt G 1995 *Phys. Rev.* B **52** 9724
[11] Riedling S *et al* 1994 *Phys. Rev.* B **49** 13283
[12] Lopez de la Torre M A, Pena V, Sefrioui Z, Arias D, Leon C, Santamaria J and Martinez J L 2006 *Phys. Rev.* B **73** 052503
[13] Svedlindh P *et al* 1989 *Physica* C **162–164** 1365
[14] Geim A K, Dubonos S V, Lok J G S, Henini M and Maan J C 1998 *Nature* **396** 144
[15] Rice T M and Sigrist M 1997 *Phys. Rev.* B **55** 14647
[16] Thompson D J, Minhaj M S M, Wenger L E and Chen J T 1995 *Phys. Rev. Lett.* **75** 529
[17] Kostic' P, Veal B, Paulikas A P, Welp U, Todt V R, Gu C, Geiser U, Williams J M, Carlson K D and Klemm R A 1996 *Phys. Rev.* B **53** 791
[18] Koshelev A E and Larkin A I 1995 *Phys. Rev.* B **52** 13559

[19] Moshchalkov V V, Qiu X G and Bruyndoncx V 1997 *Phys. Rev.* B **55** 11793
[20] Chaban A 2000 *J. Supercond.* **13** 1001
[21] Drachuck G, Shay M, Bazalitsky G, Berger J and Keren A 2012 *Phys Rev.* B **85** 184518
[22] Leviev G I, Genkin V M, Tsindlekht M I, Felner I, Paderno Y B and Filippov V B 2005 *Phys. Rev.* B **71** 064506
[23] Werthamer N R, Helfand E and Hohenberg P C 1966 *Phys. Rev.* **147** 295
[24] Wang Y and Wen H-H 2008 *Eur. Phys. Lett.* **81** 57007
[25] Tsindlekht M I, Leviev G I, Genkin V M, Felner I, Mikheenko P and Abell J S 2006 *Phys. Rev.* B **74** 132506
[26] Wang Y, Li L and Ong N P 2006 *Phys. Rev.* B **73** 024510
[27] Tsindlekht M I, Genkin V M, Leviev G I and Shitsevalova N Yu 2010 *J. Phys.: Condens. Matter* **22** 095701
[28] Tsindlekht M I, Leviev G I, Genkin V M, Felner I, Paderno Yu B and Filippov V B 2006 *Phys. Rev.* B **73** 104507